Microclimate affects soil chemical and mineralogical properties of cold alpine soils of the Altai Mountains (Russia)

Egli, Markus ; Lessovaia, Sofia N ; Chistyakov, Kirill ; Inozemzev, Svyatoslav ; Polekhovsky, Yurii ; Ganyushkin, Dmitry

Abstract: Purpose: The present work focuses on cold alpine soils of the Altai Mountains (Siberia, Russia). Permafrost is widespread and often occurs at a depth of about 100 cm. The area is characterised by extremely cold winters and cool summers: the aim was consequently to find out whether weathering could be more intense on thermally less unfavoured conditions or whether the abundance of water could be a more important factor. Materials and methods: We investigated 10 soils in a very small area close to a local glacier tongue. Five of the investigated soils were south-facing and the other five north-facing. The soils have the same parent material (mica-rich till), altitude, topography and soil age. The vegetation is alpine grassland that is partially intersected with some juniper and mosses. Soil chemical properties such as organic C, N, soil organic matter quality (using DRIFT), pH value, (oxy)hydroxides, total elemental contents (XRF) and soil micromorphology and mineralogy (using diagnostic treatments and XRD) were determined. The age constraint of the site was given by geomorphic studies together with 14C dating of a nearby peat bog and the stable organic matter fraction of the soils. Results and discussion: The soils have a Holocene age. The results showed astonishingly clearly—similarly to the European Alps—that the north-facing soils have a higher weathering state. This is expressed by lower pH values, higher oxalate and dithionite extractable Fe, Al, Mn and Si contents, higher C and N concentrations and stocks when compared to the south-facing sites. No statistically significant differences with respect to weathering indexes could be detected. The geochemical evolution of the soils seems to be enhanced at north-facing sites, even though very severe climatic conditions prevail. Furthermore, biodegradation seems to be less pronounced on north-facing compared to south-facing sites as poorly degraded organic matter is accumulated. This gives rise to more organic ligands that promote metal binding and their subsequent eluviation along the soil profile. Conclusions: We consequently must assume that weathering is not limited by low temperatures in the active layer but is rather controlled by soil moisture that seems to be higher during the warmer period in the north-facing soils.

DOI: https://doi.org/10.1007/s11368-013-0838-4

DOI: https://doi.org/10.1007/s11368-013-0838-4

J Soils Sediments (2015) 15:1420–1436
DOI 10.1007/s11368-013-0838-4

SOIL FORMATION AND WEATHERING IN TIME AND SPACE

Microclimate affects soil chemical and mineralogical properties of cold alpine soils of the Altai Mountains (Russia)

Markus Egli · Sofia N. Lessovaia · Kirill Chistyakov · Svyatoslav Inozemzev · Yurii Polekhovsky · Dmitry Ganyushkin

Received: 20 October 2013 / Accepted: 17 December 2013 / Published online: 11 January 2014

Abstract
Purpose The present work focuses on cold alpine soils of the Altai Mountains (Siberia, Russia). Permafrost is widespread and often occurs at a depth of about 100 cm. The area is characterised by extremely cold winters and cool summers: the aim was consequently to find out whether weathering could be more intense on thermally less unfavoured conditions or whether the abundance of water could be a more important factor.
Materials and methods We investigated 10 soils in a very small area close to a local glacier tongue. Five of the investigated soils were south-facing and the other five north-facing. The soils have the same parent material (mica-rich till), altitude, topography and soil age. The vegetation is alpine grassland that is partially intersected with some juniper and mosses. Soil chemical properties such as organic C, N, soil organic matter quality (using DRIFT), pH value, (oxy)hydroxides, total elemental contents (XRF) and soil micromorphology and mineralogy (using diagnostic treatments and XRD) were determined. The age constraint of the site was given by geomorphic studies together with ^{14}C dating of a nearby peat bog and the stable organic matter fraction of the soils.
Results and discussion The soils have a Holocene age. The results showed astonishingly clearly—similarly to the European Alps—that the north-facing soils have a higher weathering state. This is expressed by lower pH values, higher oxalate and dithionite extractable Fe, Al, Mn and Si contents, higher C and N concentrations and stocks when compared to the south-facing sites. No statistically significant differences with respect to weathering indexes could be detected.

The geochemical evolution of the soils seems to be enhanced at north-facing sites, even though very severe climatic conditions prevail. Furthermore, biodegradation seems to be less pronounced on north-facing compared to south-facing sites as poorly degraded organic matter is accumulated. This gives rise to more organic ligands that promote metal binding and their subsequent eluviation along the soil profile.
Conclusions We consequently must assume that weathering is not limited by low temperatures in the active layer but is rather controlled by soil moisture that seems to be higher during the warmer period in the north-facing soils.

Keywords Clay minerals · Organic carbon · Oxyhydroxides · Permafrost · Water availability · Weathering

Responsible editor: Arnaud Temme

M. Egli (✉)
Department of Geography, University of Zurich, Winterthurerstrasse 190, Zurich 8057, Switzerland
e-mail: markus.egli@geo.uzh.ch

S. N. Lessovaia · K. Chistyakov · S. Inozemzev · D. Ganyushkin
Faculty of Geography and Geoecology, St. Petersburg State University, V.O. 10 line d 33, St. Petersburg 199178, Russia

S. N. Lessovaia
e-mail: lessovaia@yahoo.com

Y. Polekhovsky
Geological Faculty, St. Petersburg State University, Universitetskaya nab., 7/9, St. Petersburg 199034, Russia

1 Introduction

Precipitation and temperature particularly influence soil properties by affecting the type and rates of chemical, biological and physical processes (Dahlgren et al. 1997; Birkeland 1999). Vegetation growth and decomposition, which depend on temperature and the other environmental factors, influence weathering reactions through the production of acidity and organic ligands that may promote chemical weathering and subsequent elemental leaching. Weathering rates, in general, are not only driven by climate as known from the paradigm of Dokuchaev (1883) and, in an extended form, of Jenny (1941).

Chemical weathering intensities depend on (i) the lithology (e.g. highly reactive minerals such as carbonates and sulphates versus crystalline rocks; see, e.g. Simas et al. (2006)), (ii) biology (Gorbushina 2007) and the development of organic matter (Conen et al. 2007), (iii) the topography and—related to it—the rate of supply of fresh regolith through physical weathering and erosion (Dixon et al. 2012; Dixon and von Blanckenburg 2012), (iv) the age of exposure and (v) the character of the hydrological system.

Several studies have shown the influence of slope aspect and the resulting microclimate on soil weathering and development (Klemmedson 1964; Macyk et al. 1978; Carter and Ciolkosz 1991; Rech et al. 2001; Egli et al. 2007). Slope aspect is directly related to the incoming solar energy, particularly relevant for permafrost-affected soils of continental climate (Osawa et al. 2010). There is no doubt that temperature (energy) determines mineral and soil weathering—even in the long-term over thousands of years as shown by Williams et al. (2010). Nevertheless, there is no unanimous agreement whether weathering in cold regions is driven more by the temperature or the availability of water (White and Blum 1995; White et al. 1999; Egli et al. 2006; 2011; Dixon et al. 2009; Williams et al. 2010; Rasmussen et al. 2011; etc.). As shown by previous investigations in the European Alps (Egli et al. 2008), higher temperatures do not necessarily lead to higher weathering rates in cold alpine regions. Water fluxes through the soils seem to be at least equally important. In general terms, the explanation of weathering in cold regions often identified three basic tenets (Hall et al. 2002): (i) weathering is dominated by mechanical processes, (ii) the predominant mechanical process is freeze–thaw and (iii) due to the low temperatures, chemical weathering is not a significant element of cold region processes. Hall et al. (2002) showed that even at low temperature, weathering rates can be high.

The scope of this paper was thus to test if the hypothesis that moisture availability predominantly determines weathering can also be applied to a very cold region having extreme climatic conditions. In order to accomplish this, the soils must have (almost) identical conditions (parent material, age, climate in general, vegetation and topography).

2 Study site

To tackle the above-mentioned scope and to test the hypothesis, the sites had to meet the criteria of having a cold climate (in a permafrost region), of showing within short distances north- and south-exposure (leading to a difference in solar energy) and of not being too old (thus avoiding the risk that too many warmer and colder periods could have disturbed the system). Weathering of primary rocks is faster on relatively young surfaces (Mavris et al. 2010). Consequently, differences between north- and south-facing sites should be better assignable to thermal differences. The investigated field sites (2,380 m asl) are located in the south-eastern part of the Altai Mountains (border region: Russia/Mongolia/China) at 49°49.159′N, 87°50.912′E and are found in an extended proglacial area of the Sophiysky Glacier of the South Chuya Ridge (Fig. 1). The tendency of glacier degradation since the end of the 19th century is to be at an average rate of 15–20 m per year (Ostanin et al. 2004). The Sophiysky Glacier has retreated 18 m per year over the last 100 years; the altitude of its tongue was 2,485 m asl in 2000 (Agatova et al. 2002). In the Altai Mountains, meteorological stations are mostly found at altitudes<1,000 m asl. Only two are at>2,000 m asl (located in highland) and four are at an altitude between 1,000 and 2,000 m asl. The annual variation of temperature is in general strongly pronounced. In the highlands, the absolute minimum temperature is around −50 to −56 °C (Marinina and Samoilova 1987). The nearest meteorological station is Kosh-Agach (1,830 m asl) that is situated about 55 km east of the investigation site where a minimum air temperature of −62 °C was recorded in 1969 (Narozhniy and Zemtsov 2011). Average soil surface temperature in January there is −30 °C. As an average over the last few decades, a snow cover was measured there for 131 days per year (Osokina et al. 1993). Average snow cover is quite low with 10 cm (which enhances the production of permafrost). According to the geobotanical zonation (Ogureeva 1980), the studied area belongs to the alpine–tundra altitudinal belt (at a height of 2,400–3,200 m asl) of the Chuya–Argutskey region of the Central Altai sub-province. Typical for this region are meadows and mountainous tundra. Average mean summer temperature varies between +9 and +2.0 °C at the lower part (see also Narozhniy and Zemtsov 2011) of the zonal belt to about +5 to 1.1 °C in the upper part. Mean annual precipitation is 550–1,000 mm (Syromyatina 2010). The studied area is located at the boundary between semi-humid and semi-arid mountainous climates. The soil temperature regime is gelic (IUSS Working Group WRB, 2007).

The studied area is located on a ledge—a small ridge (2–3 ha) that crosses the Akkol River. The ridge is covered by moraine sediments. The distance from the glacial tongue is~4 km. Mostly gneiss-like stones are found close to the edge of the glacier while, on the bank of the river opposite to the ridge, rocks having an alkaline composition are also found.

3 Material and methods

3.1 Sampling strategy

The area of interest was small and covered about 2–3 ha. Soil material was collected from excavated profile pits in

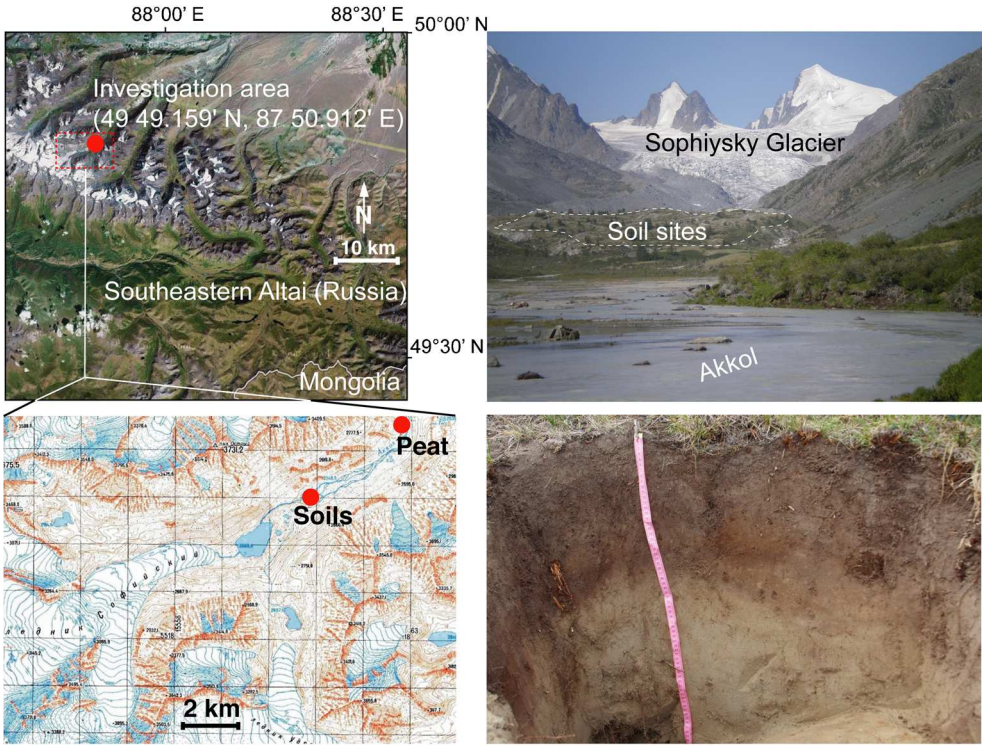

Fig. 1 Location of the study sites (soils and peat bog) in the southeastern part of the Altai Mountains (border region: Russia/Mongolia/China). Impression of the environment and sampling sites together with a typical soil profile

undisturbed locations. All sites were fully covered with vegetation. The vegetation is alpine grassland that is partially intersected with some juniper and mosses. Five soils on the north-facing and five soils on the south-facing slope were sampled at a depth of 0–15 and 15–30 cm. In addition, a soil profile including also the BC horizon was dug. They showed the following horizon differentiation: weakly decomposed litter (0–5 cm), a humus horizon A (5–19 cm), an ABw (19–27 cm) horizon that was characterised by a gradual decrease of colour intensity and a BC horizon (27–68 cm). Due to the presence of permafrost (often at a depth of about 0.5 to 1.5 m) and some cryogenic features (frost heave), the soils can all be classified as Cambic Cryosols (Table 1). They exhibited a sandy-silt texture (Table 2). Furthermore, some rock fragments in the soil profile and a hard rock (gneiss) in the bank of the Akkol River (opposite to the ridge) were sampled to determine the possible mineral source for soils.

One to two kilograms soil material per sample was taken for the analyses (Hitz et al. 2002). The bulk density (fine earth and soil skeleton) was measured on undisturbed samples.

Furthermore, two samples from a peat bog were taken and dated in order to have an additional time constraint of the surface and soils. The samples were taken at the transition to the permafrost underground (approximately 1 m depth) and at a depth of 60 cm. This peat bog was located approximately 2–3 km farther down the valley. A further age indication of the surface was obtained from two soil samples of the investigated site by dating the stable organic matter fraction (resistant to an H_2O_2 treatment; see Favilli et al. 2008).

3.2 Soil chemical and physical analyses

Total C and N contents of the soil were measured with a C/H/N analyser (Elementar Vario EL). Soil pH (in 0.01 M $CaCl_2$) was determined on air-dried fine earth samples using a soil:solution ratio of 1:2.5. As the soils did not contain inorganic carbon, the total C content equals the organic carbon content. LOI (loss-on-ignition) was determined on 2.5 g soil material ignited at 950 °C during 3 h.

After a pre-treatment of the samples with H_2O_2 (3%), particle size distribution of the soils was measured using a combined method consisting of sieving the coarser particles (2,000–32 μm) and the measurement of the finer particles (<32 μm) by means of an X-ray sedimentometer (SediGraph 5100).

Oven-dried (70 °C) samples were sieved to<2 mm. Fe, Al, Mn and Si concentrations were determined after treatment with NH_4-oxalate (buffered at pH 3, labelled 'o') (McKeague et al. 1971). The extracts were centrifuged for 8 min at 4,000 rpm and filtered (mesh size 0.45 μm, S&S, filter type 030/20). Element concentrations were measured using atomic absorption spectroscopy (AAnalyst 700, PerkinElmer). The oxalate treatment extracts both the weakly and poorly crystalline phases and some of the organic phases, but normally does not dissolve the strong humus–metal complexes (Mizota and van Reeuwijk 1989). Additionally, the dithionite (Mehra and Jackson 1958) was measured for the elements Fe and Al.

Table 1 Characteristics of the study sites

Site	Exposure (°N)	Slope (degree)	Altitude (m asl)	Parent material	Vegetation	Soil group (IUSS Working Group WRB, 2007)
North-facing sites						
3	340	10	2,378	Glacial deposits; silt loam or loam	Alpine grassland	Cambic Cryosol
4	0	8	2,378	Glacial deposits; silt loam or loam	Alpine grassland	Cambic Cryosol
5	8	14	2,376	Glacial deposits; silt loam or loam	Juniper, Alpine grassland	Cambic Cryosol
6	10	6	2,376	Glacial deposits; silt loam or loam	Juniper, Alpine grassland	Cambic Cryosol
7	303	7	2,382	Glacial deposits; silt loam or loam	Alpine grassland	Cambic Cryosol
South-facing sites						
8	195	13	2,383	Glacial deposits; silt loam or loam	Alpine grassland	Cambic Cryosol
9	155	9	2,379	Glacial deposits; silt loam or loam	Alpine grassland	Cambic Cryosol
10	154	12	2,376	Glacial deposits; silt loam or loam	Alpine grassland	Cambic Cryosol
11	154	12	2,376	Glacial deposits; silt loam or loam	Alpine grassland	Cambic Cryosol
12	130	10	2,376	Glacial deposits; silt loam or loam	Alpine grassland	Cambic Cryosol

The sites are within an area of about 2–3 ha

Table 2 General physical and chemical characteristics of the soil material

Site	Depth (cm)	Skeleton content (weight %)	Bulk density (g/cm^3)	Sand (%)	Silt (%)	Clay (%)	Texture	pH ($CaCl_2$)	C (g/kg)	N (g/kg)	C/N
North-facing											
Alt 3	0–15	0.3	0.90	46.7	46.2	7.1	L	5.2	41.40	2.86	14.5
Alt 3	15–30	0.0	0.95	54.6	39.0	6.4	SL	5.1	21.30	1.63	13.1
Alt 4	0–15	0.2	0.92				SiL	5.0	30.69	2.25	13.6
Alt 4	15–30	0.2	1.05				SiL	5.1	22.83	1.78	12.9
Alt 5	0–15	0.0	0.83	35.5	51.4	13.1	SiL	4.4	47.09	2.70	17.4
Alt 5	15–30	0.0	0.79	26.6	63.4	10.0	SiL	4.5	49.92	3.08	16.2
Alt 6	0–15	0.0	0.73				SiL	4.4	43.90	2.55	17.2
Alt 6	15–30	0.0	1.10				SiL	4.5	19.11	1.07	17.9
Alt 7	0–15	0.1	1.17				SiL	4.7	22.41	1.74	12.9
Alt 7	15–30	0.0	0.97				SiL	5.4	22.22	1.64	13.5
South-facing											
Alt 8	0–15	0.1	0.98	38.4	51.2	10.4	SiL	5.6	22.49	1.81	12.4
Alt 8	15–30	0.1	0.93	50.2	43.5	6.3	L	6.1	20.96	1.68	12.5
Alt 9	0–15	0.0	1.08				SiL	5.0	16.54	1.39	11.9
Alt 9	15–30	0.0	0.95				SiL	5.2	15.15	1.36	11.1
Alt 10	0–15	0.8	0.91	40.9	51.8	7.7	SiL	5.4	20.63	1.61	12.8
Alt 10	15–30	0.1	0.95	29.6	62.3	8.1	SiL	5.7	12.24	1.04	11.8
Alt 11	0–15	0.0	1.00				SiL	5.3	29.56	2.16	13.7
Alt 11	15–30	0.0	1.20				SiL	5.2	14.69	1.14	12.9
Alt 12	0–15	0.1	0.89				SiL	4.5	29.99	2.27	13.2
Alt 12	15–30	0.0	0.99				SiL	5.4	27.65	2.10	13.2
Profile/horizon											
A	5–19	0.2	0.92				SiL	5.2	31.19	2.60	12.0
ABw	19–27	0.2	1.05				SiL	5.1	36.41	2.92	12.5
BC	27–68	0.1	1.10				SiL	4.9	6.62	0.43	15.4

SiL Silt loam, *SL* sandy loam, *L* loam

Measurement of the total element content of fine earth and skeleton was done by means of X-ray fluorescence (XRF). Approximately 10 g of soil material was milled to<50 μm in a tungsten carbide disc swing mill (Retsch® RS1, Germany). Four grams of soil powder was mixed with 0.9 g of Licowax® C Micro-Powder PM (Clariant, Switzerland), pressed into a 32-mm pellet and analysed using an energy-dispersive X-ray fluorescence spectrometer (SPECTRO X-LAB 2000, SPECTRO Analytical Instruments, Germany).

3.3 Weathering indexes

Several indexes have been defined to characterise chemical weathering in soils. The general principle of all these indexes is similar and based on the ratio of the base cations (Ca, Mg, K, Na) to Al and/or Si. We used the 'index A' and 'index B' of Kronberg and Nesbitt (1981). These indexes are defined by the molar ratio of

$$A = \frac{SiO_2 + CaO + K_2O + Na_2O}{Al_2O_3 + SiO_2 + CaO + K_2O + Na_2O} \quad ; \qquad B = \frac{CaO + K_2O + Na_2O}{Al_2O_3 + CaO + K_2O + Na_2O} \tag{1}$$

In addition, also the CIA and CIW indexes were tested (Harnois 1988; Nesbitt and Young 1989):

$$CIA = \frac{Al_2O_3}{Al_2O_3 + CaO + Na_2O + K_2O} \quad ; \qquad CIW = \frac{Al_2O_3}{Al_2O_3 + CaO + Na_2O} \tag{2}$$

The molar ratio of (K+Ca)/Ti is used as a 'dating' method for rock varnish in semi-arid to arid regions (Harrington and Whitney 1987). As Ti is considered to be an immobile element, the ratio can be used as a weathering index: the lower the ratio, the higher the degree of weathering.

3.4 Stock calculations of C, N and oxyhydroxides

The oxalate-extractable Fe_o, Al_o, Si_o, Mn_o and C and N stocks were calculated according to the following equation:

$$E_{stock} = \sum_{a=1}^{n} E_i \Delta z_i \rho_i (1 - RM) \tag{3}$$

where E_{stock} denotes the elemental abundance (kg/m^2), E the elemental concentration (kg/t), Δz_i the thickness of layer i (m), ρ the soil density (t/m^3) and RM the mass proportion of rock fragments.

3.5 Micromorphology and X-ray diffractometry

The rock samples from the soil horizons were studied in thin sections by optical microscopy using Zeiss Axioplan 2 and Polam P-312 microscopes. The micromorphological study of soil horizons was performed using thin sections and an Olympus optical microscope. The fine earth (<2 mm fraction), the rock fragments and the gneiss were analysed as random samples using X-ray diffraction (MiniFlex ii (Rigaku), CoKα radiation).

After dispersion of the sample by adding some drops of ammonia as peptising agent, the<1-μm fraction was separated from the soil material by sedimentation and decantation. Some drops of ammonia as peptising agent were added for dispersion of the soil sample. The mineralogical composition of the<1-μm fraction was studied on oriented specimen using X-ray diffractometry (XZG-4A Carl Zeiss Jena) with CuKα radiation and a monochromator in the diffracted beam. Prior to XRD analysis, the following diagnostic treatments were performed: (i) saturation with Mg, (ii) ethylene glycol solvation and (iii) heating at 550 °C for 3 h. Digitised X-ray data were corrected for Lorentz and polarisation factors (Moore and Reynolds 1997). To better detect single minerals and mixed-layered phases, diffraction patterns were fitted by the Origin™ PFM program using the Pearson VII algorithm. Background values were calculated by means of a nonlinear function (polynomial second-order function; Lanson 1997).

3.6 DRIFT measurements

The samples (<2 mm fraction) used for DRIFT (Diffuse Reflectance Infrared Fourier Transform Spectroscopy) analyses were homogenised and then dried at 70 °C for 2 h (prior to analysis). Relative peak intensities were used for DRIFT analysis (Bruker, Tensor 27). Spectra were recorded from 4,000 to 250 cm^{-1}. DRIFT measurements were used to check mineralogical aspects and to estimate soil organic matter composition (functional groups).

In order to quantify the relative changes of organic-functional groups in the FT-IR spectra, we divided the values of the relative intensity (area) of each peak by the sum of the relative intensity of all the considered peaks and multiplied it by 100 using the software OPUS 6.5. An integration method was employed to calculate the relative concentration (OPUS 6.5) that used a linear background between the found bases (individual samples) and absorbance values. Major IR absorption bands and functional groups assignments are given in Table 3. Aliphatic compounds were calculated using the IR range 1,470–1,440 cm^{-1}.

Table 3 Major IR absorption bands and assignments (Piccolo and Mirabella, 1985; Stevenson, 1994; Senesi et al., 2003; Tan, 2003)

Band	Wave number cm^{-1}	Assignment
1	2,980–2,880	Aliphatic C—H stretching (aliphatic methyl and methylene groups)
2	1,725–1,710	C═O stretching of COOH, aldehydes and ketones
3	1,660–1,630	C═O stretching of amide groups, quinone C═O and/or C═O of H-bonded conjugated ketones
4	1,620–1,600	Aromatic C═C, strongly H-bonded C═O of conjugated ketones
5	1,535–1,500	Aromatic rings, amide II vibration
6	1,495–1,470	N—H stretching of proteic amides
7	1,470–1,440	Aliphatic C—H bending
8	1,413–1,333	OH deformation and C—O stretching of phenolic groups
9	1,280–1,200	C—O stretching and OH deformation of COOH, C—O stretching of aryl ethers and phenols
10	1,190–1,127	C—OH stretching of aliphatic alcohols
11	1,116–1,050	Secondary alcohols
12	1,080–1,030	C—O stretching of polysaccharides

3.7 Radiocarbon dating of organic matter fractions

The turf samples were cleaned using an acid–alkali–acid (AAA) treatment. The soil samples to be dated underwent a H_2O_2 treatment over 1 week (Favilli et al. 2008). The samples were then heated under vacuum in quartz tubes with CuO (oxygen source) to remove any absorbed CO_2 in the CuO. The tubes were then evacuated, sealed and heated in the oven at 900 °C to obtain CO_2. The CO_2 of the combusted sample was mixed with H_2 (1:2.5) and catalytically reduced over iron powder at 535 °C to elemental carbon (graphite). After reduction, the mixture was pressed into a target and carbon ratios were measured by Accelerator Mass Spectrometry (AMS) using the tandem accelerator of the Laboratory of Ion Beam Physics at the Swiss Federal Institute of Technology Zurich (ETHZ). The calendar ages were obtained using the OxCal 4.2 calibration program (Bronk Ramsey 2001; 2009) based on the IntCal 09 calibration curve (Reimer et al. 2009). Calibrated ages are given in the 2σ range (minimum and maximum value for each).

3.8 Statistics

The individual datasets were checked for normal distribution using a Shapiro–Wilk test (SigmaPlot 11.0 (Systat Software Inc.); Jann 2005). As the data did not always show a normal distribution, differences in mean values were tested using the *U*-test (Mann–Whitney). For datasets having a normal distribution, the *t*-test was applied. This procedure was checked using a two-tailed test for significance.

4 Results

4.1 Petrographic characteristics and soil micromorphology

Included rock fragments in the soil showed a polymineral and acid composition. The rock fragments were a modified biotite–plagioclase gneiss having a sub-parallel arrangement of minerals (Fig. 2a). The semi-quantitative composition was as follows: quartz 40–50%, 15–25% plagioclase, 8–10% biotite, 5–7% chlorite, 2–3% epidote, 1–2% ore mineral and leucoxene and single grains of amphiboles and tourmaline. The surface of these rocks was crossed by numerous veins having a quartz, quartz–albite and chalcedony composition (Fig. 2b). The veins reflected several generations of their formation; the last of them were chalcedony veins. Biotite was a predominant mineral among the micas. Muscovite or illite (so-called white mica) was also found but it was much less frequent. Sometimes the replacement of biotite by chlorite was identified (Fig. 2c). The studied rock initially seems to be a sedimentary rock that was later metamorphosised.

The thin sections of the soil material from the upper part of the A horizon (3–8 cm) showed samples having a loose microstructure, coarse to fine silty plasmic fabrics and a fragmentary organic-ferric plasma that is distributed like flocculus and clots (Fig. 3). The ‘coarse’ fraction was dominated by silt grains with a predominance of quartz and feldspars. In addition, biotite and hornblende were also present. Biotite particles did not show typical alteration features. However, some ferruginous flocculent films have been identified on their surface. Raw and weakly to moderately decomposed organic matter was detected. The soil material was generally slightly transformed by pedogenetic processes and weakly aggregated. The lower part of the A horizon (10–15 cm) is weakly aggregated, mainly by a silt-plasma fabric having features of zoogenic transformation. The coarse particles were mostly composed of slightly rounded quartz. Furthermore, biotite and amphiboles were found. Pedogenetic features were evident. The ABw horizon (sample from 26 to 30 cm depth) was weakly aggregated, showing a silt-plasma fabric. In general, the coarse particles showed a composition similar to that in the overlying horizon.

Similar to the other soil horizons, the BC material was weakly aggregated, having mainly a silt-plasmic fabric that was slightly transformed by pedogenetic processes. The coarse fraction was slightly rounded and composed predominantly of quartz. Compared to the other horizons, an increasing proportion of biotite was detected.

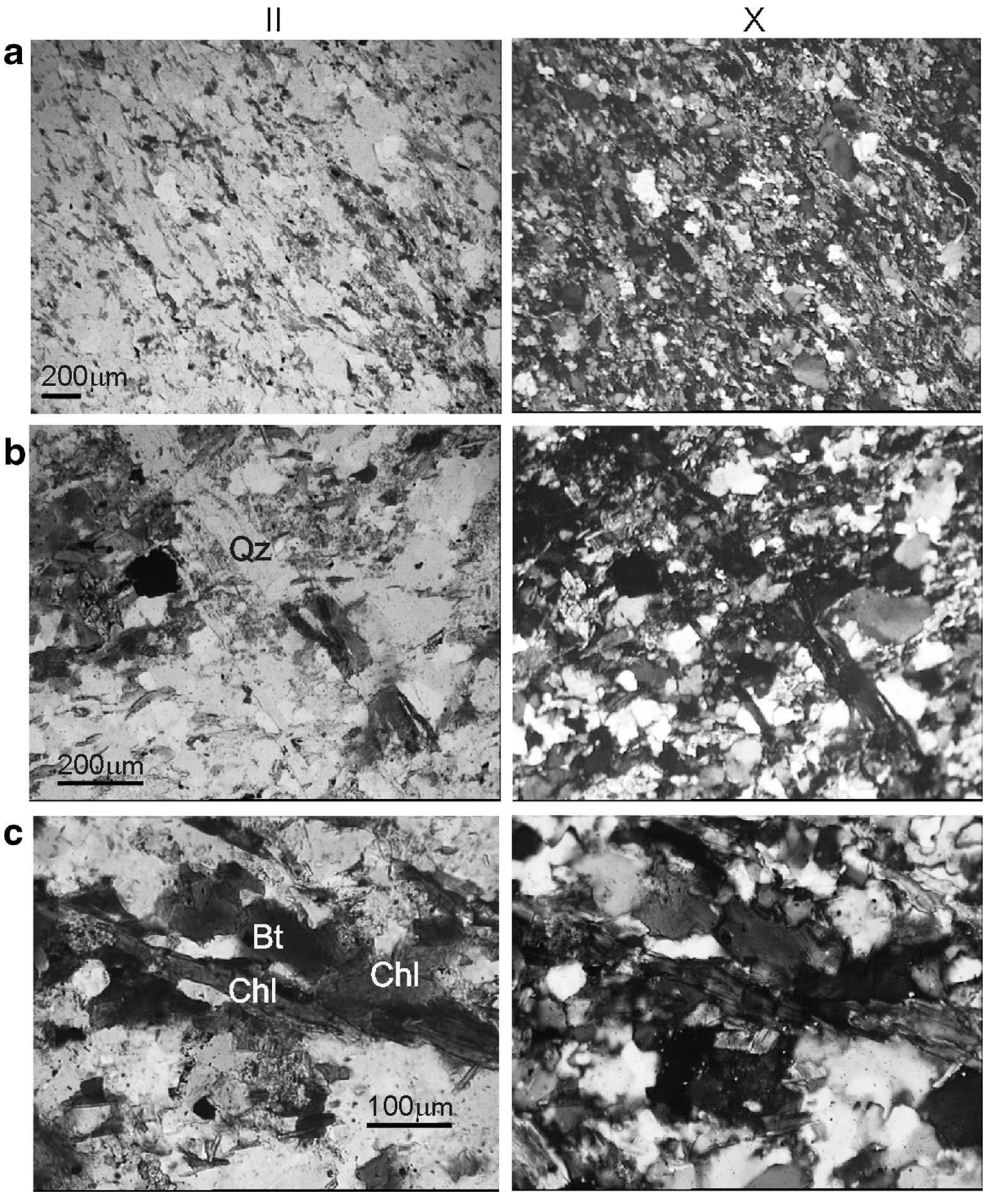

Fig. 2 Thin sections of rock samples from the soil profile: **a** gneiss structure with sub-parallel arrangement of minerals; **b** quartz vein crossing the rock; **c** development of chlorite on biotite. Determination on thin sections using (II) plain polars and (X) crossed Nicols polarised lights. Indexes are according to Whitney and Evans (2010), Qz=quartz, Chl=chlorite (group), Bt=biotite (group)

4.2 General physical and chemical soil properties

The investigated soils are acidic to moderately acidic. The pH ranged from 4.4 to 5.4 in the top layer to 6.1 in the subsoil. No carbonates were present in the soils. The grain size in all soils and horizons was similar and consisted of a sandy loam, silt loam or loam (Table 2). Typically, maximum grain size near to 120 μm was measured (data not shown). A second but much minor maximum was detectable around a grain size of 15–25 μm. Bulk density was quite uniform and varied in between 0.9 and 1.1 g/cm^3. At the north-facing sites, the C concentrations varied between 19 and 50 g C/kg and at the south-facing sites between 12 and 30 g C/kg. Similarly, the N contents were in general higher at north-facing sites (1.1–3.1 g N/kg) than at the south-facing sites (1–2.3 g N/kg). The differences between north- and south-facing sites with respect to the C and N concentrations and also the corresponding stocks (0–15, 15–30 and 0–30 cm, except N stocks) were statistically significant ($p<0.05$; Figs. 4 and 5). At north-facing sites, there was a distinct accumulation of soil organic matter. The C/N ratio of the soil organic matter varied in the range of 12.9–17.9 at north-facing and 11.1–13.7 at south-facing sites (Table 2, Fig. 4). Also here, distinct differences ($p<0.05$) between north- and south-facing sites could be measured—north-facing sites having higher C/N values.

The north-facing sites furthermore showed significantly lower pH values ($p<0.05$; Fig. 4).

4.3 Soil organic matter characteristics

The DRIFT spectra of the bulk SOM delivered information about its chemical characteristics. Independent of the

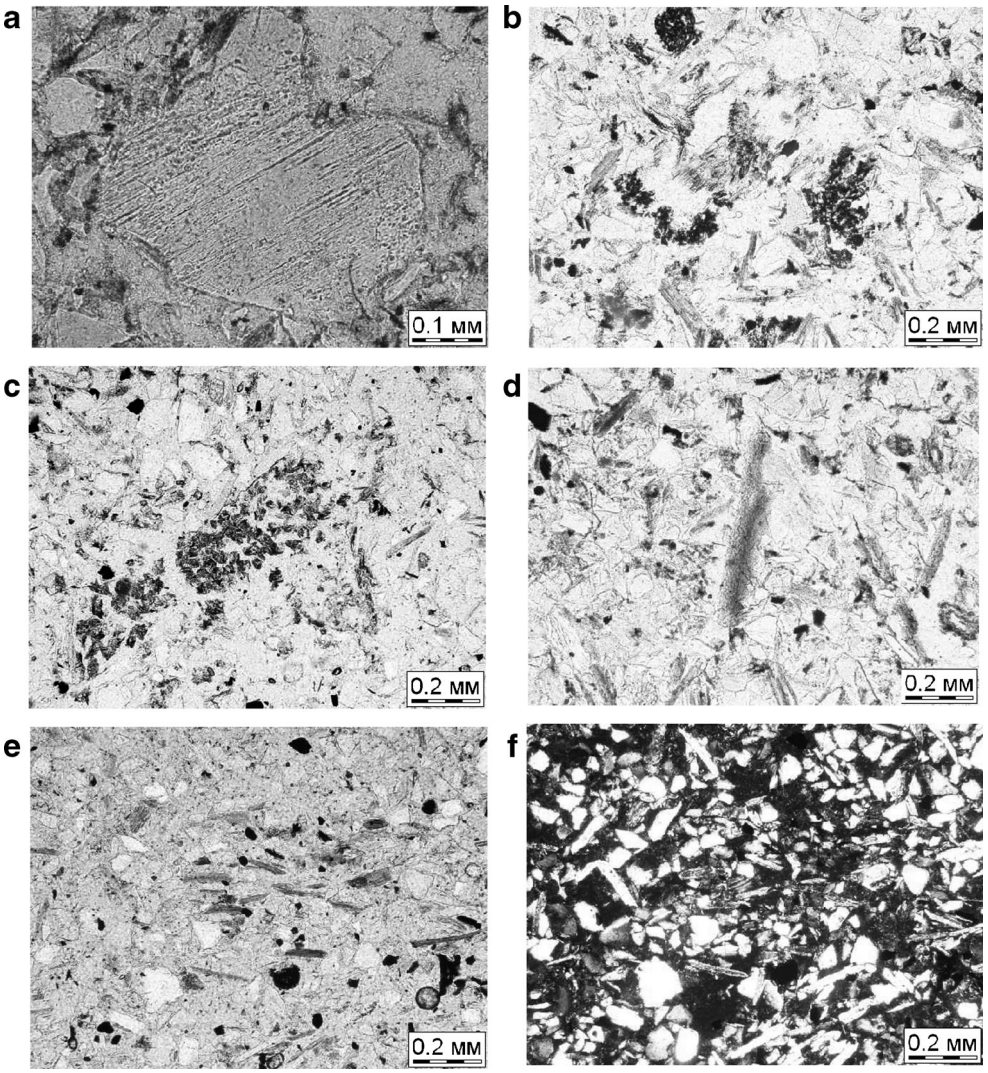

Fig. 3 Thin sections of soil samples using plain polars: **a** weakly rounded quartz grain with cleavages and frost cracks from the A horizon; **b** slightly decomposed organic matter and raw humus (A horizon); **c** fragments of zoogenic transformation (A horizon); and **d** weakly disintegrated biotite grain without features of chemical weathering (A horizon), **e** horizontally oriented biotite particles of the BC horizon and **f** sandy-silty plasmic fabric of the BC horizon using crossed Nicols

exposure, the bulk organic matter consisted mostly of aliphatic compounds (data not shown), secondary alcohols, phenolic functional groups and aromatic rings and amides and to a lesser extent of polysaccharides and other compounds.

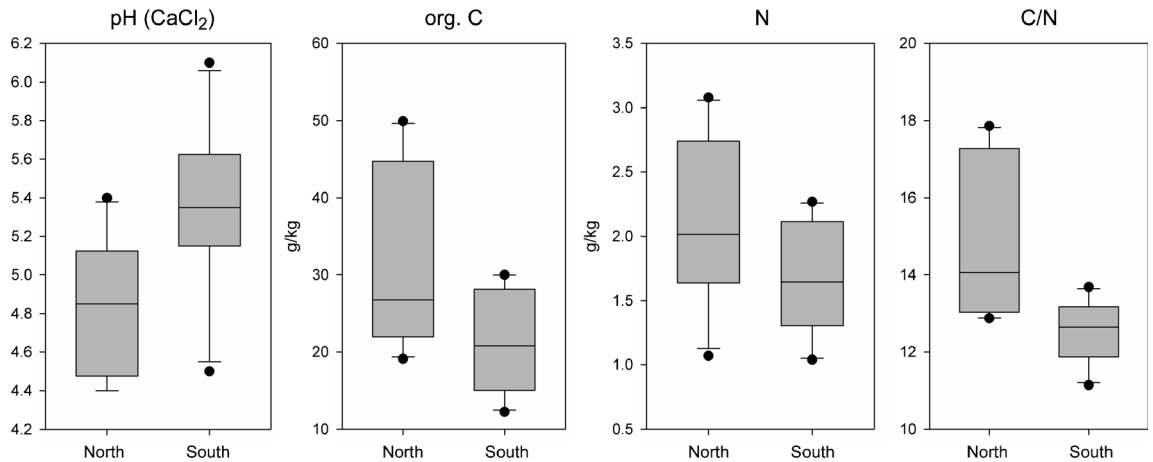

Fig. 4 Comparison (boxplot; with median, 25th- and 75th-percentile values, min and max values) of pH, organic C and N content and C/N ratio between north- and south-facing sites. The differences are significant ($p<0.05$) for pH($CaCl_2$), organic and the C/N ratio

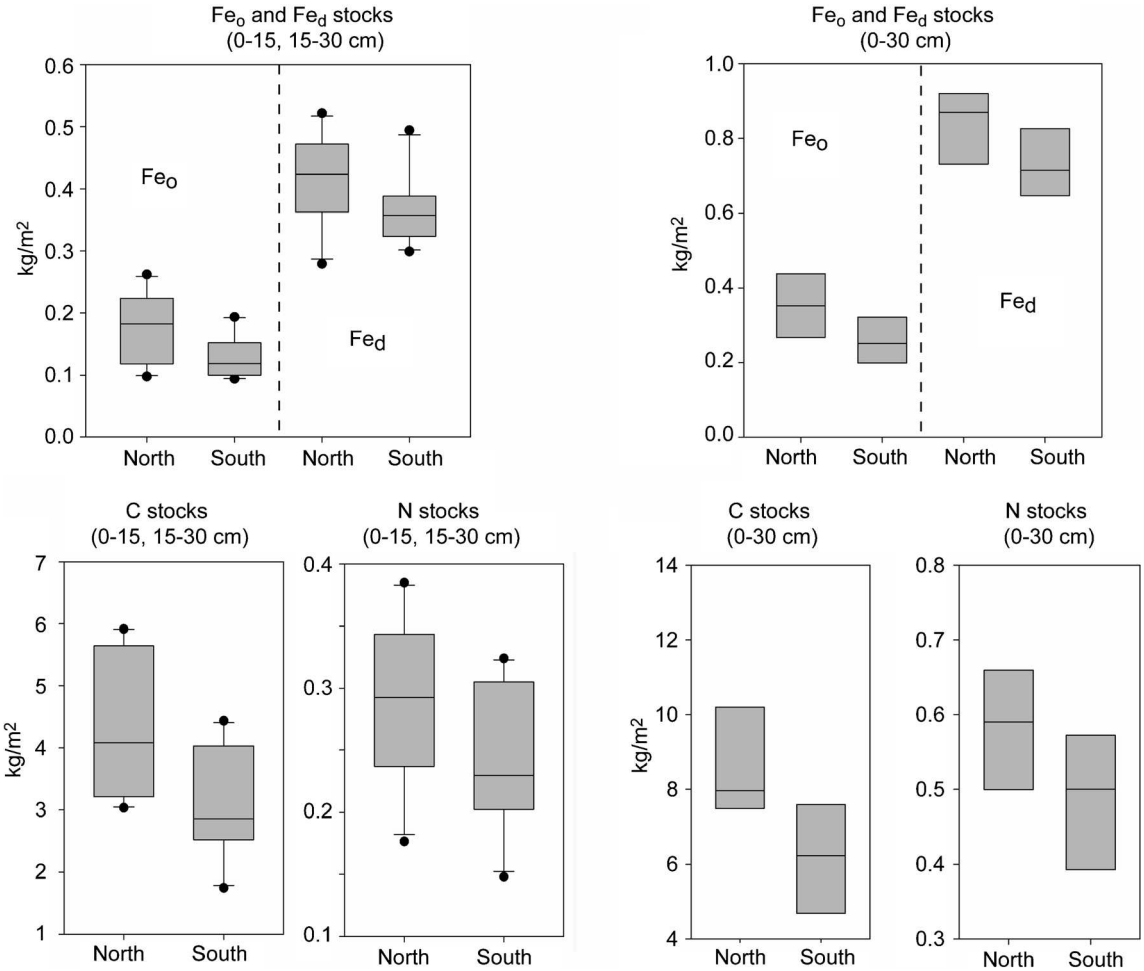

Fig. 5 Abundance (stocks) of oxyhydroxides and C and N (given for 0–15 and 15–30 and as single values of 0–30 cm soil depth) as a function of exposure. The differences are significant ($p<0.05$) for all parameters except Fe_d and N

Also regarding the chemical composition of the soil organic matter, partially distinct differences between north- and south-facing sites could be detected. North-facing sites showed a distinctly ($p<0.05$) higher relative (and absolute) proportion of carboxyl groups (—COOH) and less secondary alcohols, but a significantly higher amount of polysaccharides (Fig. 6).

Humification processes were related to the preferential oxidation of plant polysaccharides and phenolic hydroxyl groups and were further characterised by an enrichment of secondary alcohols and N-containing compounds in the SOM. The variations between the C and N contents, the C/N ratio and also the functional groups in the north- and south-facing sites would seem to indicate that there were quite distinct differences in the decomposition processes.

4.4 Pedogenetic oxyhydroxides

The oxalate- and dithionite-extractable contents are given in Table 4. The concentrations of all compounds were relatively low. The weathering stage of the soils is therefore not very advanced. In most cases the Al_o content was equal to the Al_d

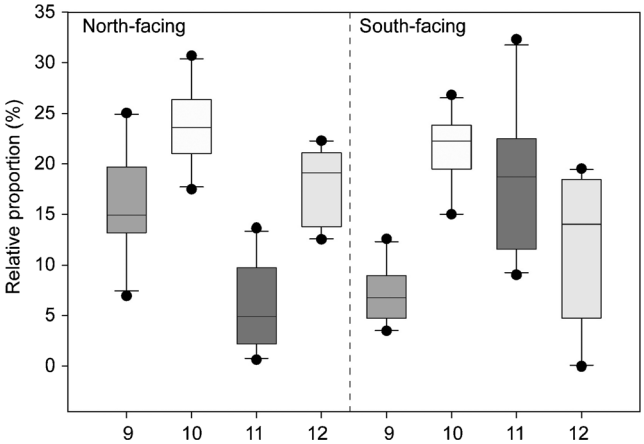

Fig. 6 Relative proportion of functional groups as a function of exposure. 9=C—O stretching and OH deformation of COOH, C—O stretching of aryl ethers and phenols; 10=C—OH stretching of aliphatic alcohols; 11= secondary alcohols; 12=C—O stretching of polysaccharides. The differences are significant ($p<0.05$) for all parameters except for 10

Table 4 Oxalate (*o*)- and dithionite(*d*)-extractable fractions of Al, Fe, Mn and Si in the fine earth

Site	Depth (cm)	Al(*o*) (g/kg)	Al(*d*) (g/kg)	Fe(*o*) (g/kg)	Fe(*d*) (g/kg)	Mn(*o*) (g/kg)	Si(*o*) (g/kg)
North-facing							
Alt 3	0–15	0.62	0.55	0.90	2.71	0.042	0.081
Alt 3	15–30	0.86	0.86	0.77	2.51	0.090	0.078
Alt 4	0–15	0.74	0.72	1.07	3.01	0.131	0.090
Alt 4	15–30	1.27	1.31	1.30	3.31	0.072	0.124
Alt 5	0–15	0.78	0.94	1.29	3.20	0.050	0.077
Alt 5	15–30	2.05	2.30	1.95	3.98	0.018	0.130
Alt 6	0–15	0.82	1.00	2.40	3.94	0.029	0.110
Alt 6	15–30	0.85	0.74	1.34	2.87	0.045	0.129
Alt 7	0–15	0.61	0.51	1.17	2.63	0.057	0.087
Alt 7	15–30	0.70	0.66	0.67	1.92	0.040	0.078
South-facing							
Alt 8	0–15	0.53	0.41	0.68	2.21	0.047	0.094
Alt 8	15–30	0.62	0.50	0.72	2.32	0.060	0.110
Alt 9	0–15	0.58	0.36	0.64	2.15	0.057	0.068
Alt 9	15–30	0.64	0.63	0.66	2.10	0.062	0.060
Alt 10	0–15	0.60	0.63	0.81	2.79	0.015	0.169
Alt 10	15–30	0.87	0.89	0.99	2.53	0.043	0.244
Alt 11	0–15	0.65	0.65	1.22	2.82	0.015	0.143
Alt 11	15–30	0.84	0.77	1.08	2.75	0.059	0.077
Alt 12	0–15	0.63	0.67	0.96	2.68	0.036	0.032
Alt 12	15–30	0.73	0.71	0.93	2.41	0.050	0.158
Profile/horizon							
A	5–19	1.01	1.05	1.36	3.23	0.065	0.104
ABw	19–27	2.04	1.85	1.78	3.76	0.077	0.174
BC	27–68	1.20	1.29	1.23	2.86	0.024	0.134

content. Sometimes the Al_o concentration exceeded Al_d which could be an indication of the presence of ITM (imogolite-type materials). The possible presence of ITM was calculated using the molar ratio Al_o/Si_o and counter-checked using DRIFT. The molar ratio should be close to 1 for allophanes and allophane-like minerals ($2SiO_2 \cdot Al_2O_3 \cdot 2.5H_2O$; Lorenzoni et al. 1995) and close to 2 for imogolite-like minerals ($SiO_2 \cdot Al_2O_3 \cdot 2.5H_2O$). The likelihood of ITM is very low if the molar ratio is<0.75 or>2.4. However, neither the DRIFT spectra nor the molar ratios (that were in the range of 3.7–20.5) gave an indication of the presence of ITM.

Similar to the pH and SOM, also here quite distinct differences, in most cases significant (except Fe_d and N), between north- and south-facing sites could be measured (Fig. 7). The concentrations of Fe_o, Fe_d, Al_o, Al_d, Mn_o and also the corresponding stocks were significantly (except Fe_d) higher at the north-facing sites (Table 4, Figs. 5 and 7) and indicated a more intense weathering and a higher release of metals (Zanelli et al. 2007). The Fe_o/Fe_d ratio was also higher at north-facing sites showing the formation of iron oxides with a lower degree of crystallinity; this reflects the effect of the higher content of organics that impede the crystallization of iron oxides (Cornell and Schwertmann 2003).

4.5 Mineralogy of the fine earth and clay fraction

Using the DRIFT spectra, an approximate and general mineralogical characterisation of all soil samples (fraction<2 mm) was made possible. Various regions in the IR spectrum contained OH vibrational information. In the OH-bending and M—O region (1,200–300 cm^{-1}), the bands associated with hydroxyl groups could be discriminated from each other, and band assignment is straightforward. Furthermore, this region is not affected by the presence of residual water molecules (Vantelon et al. 2001). Additional indications, in some cases straightforward, can be obtained from the OH-stretching region (4,000–3,000 cm^{-1}). In all samples, primary minerals such as quartz and mica and to a lesser extent muscovite could be detected. Quartz was identified based on 1,164 and 1,080 cm^{-1} Si—O asymmetrical stretching vibrations, the typical doublet at 800 and 780 cm^{-1} (Si—O symmetrical stretching vibrations), the 700-cm^{-1} Si—O symmetrical bending vibrations and the 514- and 465-cm^{-1} Si—O asymmetrical bending vibration (Hlavay et al., 1978). The vibration at 3,624 cm^{-1} indicated the presence of dioctahedral silicate (Madejova and Komadel, 2005), probably dioctahedral mica as suggested by the micromorphology analyses (Fig. 8). In many samples, some kaolinite was discernible (based on weak absorptions at 3,694 cm^{-1} using DRIFT). As a weathering product, some gibbsite seemed also to be present. In most samples, some chlorite was also detected (although the chloritic phases may comprise weathering products such as HIV). Often a peak near 670 cm^{-1} was detectable: this points to the 2:1 layer either in talc (Schroeder 2002; Kloprogge et al. 2004) or epidote (Langer and Raith 1974). The chloritic components and epidote (or the probable presence of talc) point to a small admixture of basic material. The material that derives from the adjacent valley slopes was interspersed (glacial abrasion) during glacial advance with the gneissic glacial material that derived from the upper part of the valley.

The XRD patterns (Fig. 8) of the fine earth (the <2-mm fraction) revealed the following minerals (for all soil horizons): (i) chlorite (peaks with *d* values of 1.42, 0.71, 0.47 (very minor peak, not indicated in the XRD pattern), 0.35 nm, etc.) and (ii) mineral(s) of the mica group (1.00; 0.50). The peak at 0.389 nm denotes muscovite (Brindley and Brown, 1980), (iii) feldspars (0.64, 0.404, 0.377 nm etc.) and (iv) quartz (0.425, 0.344, 0.229, 0.224 nm, etc.). The peak with a *d* value of 0.85 nm could be attributed to amphibole.

When comparing the XRD peak intensity, a relative decrease of chlorite and mica towards the surface could be detected. Mica seems to show the lowest concentration in

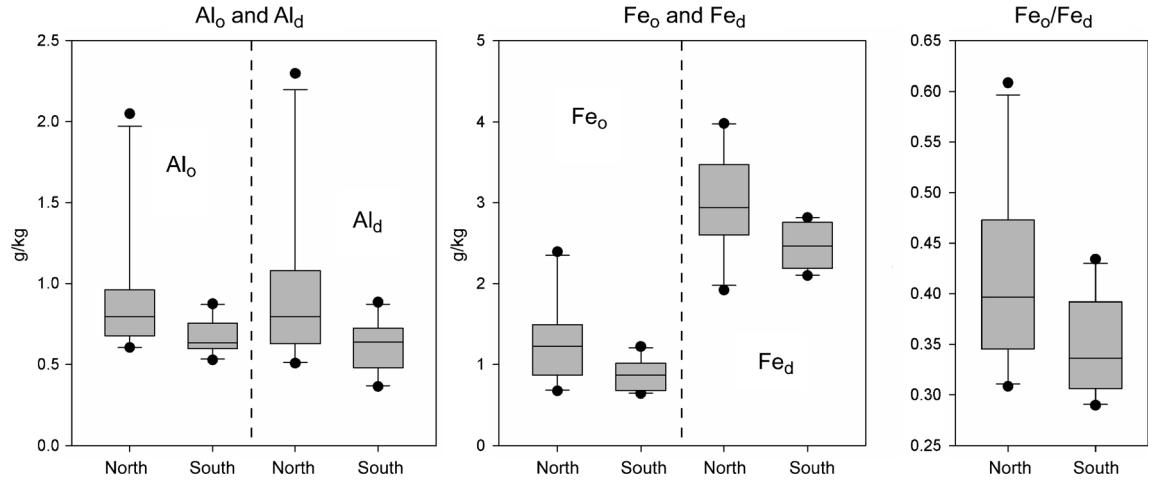

Fig. 7 Comparison (box plot; with median, 25th- and 75th-percentile values, min and max values) of the dithionite- and oxalate-extractable fractions and Fe_o/Fe_d ratio between north- and south-facing sites. The differences are significant ($p<0.05$) for all parameters except Al_o and Fe_o/Fe_d

the ABw horizon. Chlorite, mica, feldspar, quartz and traces of amphibole were also found in the gneiss (rock sample of the river bank) and the rock fragments in the soil. Some variability could be measured regarding the mica and chlorite proportion (Fig. 8).

In all samples, chlorite was iron rich because of the ratio of odd to even peaks: the *d*(002) 0.71 nm and *d*(004) 0.354 nm peaks are considerably higher than the *d*(001) 1.42 nm and *d*(003) 0.472 nm peaks (Moore and Reynolds, 1997). The contribution of kaolinite to the 0.71 nm peak was low, as evidenced by its weak absorption at 3,694 cm^{-1} in the DRIFT spectra.

In the fine-size fraction (<1 μm), chlorite and biotite were identified by XRD, as were also the products of biotite transformation represented by mixed-layered biotite–vermiculite having a minor proportion of vermiculitic layers. Chlorite was identified based on the d_{001} and d_{003} reflections at 1.40 nm and 0.471–0.473 nm, respectively. The d_{001} reflection at 1.40 nm, in fact, remained stable after ethylene glycol solvation and showed a slight contraction to 1.38 nm after heating at 550 °C. Mica group minerals were detected for their d_{001} and d_{002} basal reflections at 1.00 nm, which remained stable after the ethylene glycol and heating treatments. The low intensity of the peak at 0.50 nm, in the fine earth random samples, indicated a trioctahedral nature of this mineral. Together with the results of the thin sections, mica could be classified as biotite. The weathering product of biotite was a mixed-layered biotite–vermiculite having a minor proportion of vermiculite. The mixed-layered clay minerals were recognised by the asymmetries towards lower angles of the 1.00 nm peak of the XRD patterns of the Mg-saturated samples. No shift of these peaks occurred after ethylene glycol solvation (consequently, smectitic weathering products were not present). In the clay-size fraction≤1 μm, biotite and chlorite were found in all horizons. Compared to the other horizons, the proportion of mixed-layered biotite–vermiculite seemed to be highest in the ABw horizon (Fig. 8).

4.6 Total elemental contents and weathering indexes

The total elemental contents reflect the gneissic/granitic character of the soil material with SiO_2 contents between 65 and 69% (Table 5). The concentration of base cations (Ca, Mg, K and Na) is relatively high.

The molar ratio of (K+Ca)/Ti is used as a dating method for rock varnish in semi-arid to arid regions (Harrington and Whitney 1987). As Ti is considered to be an immobile element, the ratio can be used as a weathering index: the lower it is, the higher the degree of weathering. The comparison between north- and south-facing sites is given in Fig. 9. Although the differences seem to be small and not significant, a slight trend towards a lower ratio at north-facing sites can be measured. A similar observation is made for the A and B indexes. Particularly for the A index, a (nonsignificant) trend towards lower values at north-facing sites can be detected (Fig. 9). It seems that a stronger enrichment of Al over Ca, K and Na occurs at the north-facing sites.

4.7 Age of the sites

There is no detailed geomorphic mapping of the area of interest. The sites are in between the maximum extent of the glacier during the Little Ice Age and the Late Glacial position of the moraines (Younger and Oldest Dryas). Consequently, the surface of interest has been exposed to weathering in the time span>200 years and<15 kyr. Some more detailed age indications are obtained by the dating of a nearby peat bog that gives a minimum age of 1,304–1,415 years cal BP (Table 6). The stable soil organic matter has a maximum age of 5,317–5,468 cal BP. With this, the age of the soils can

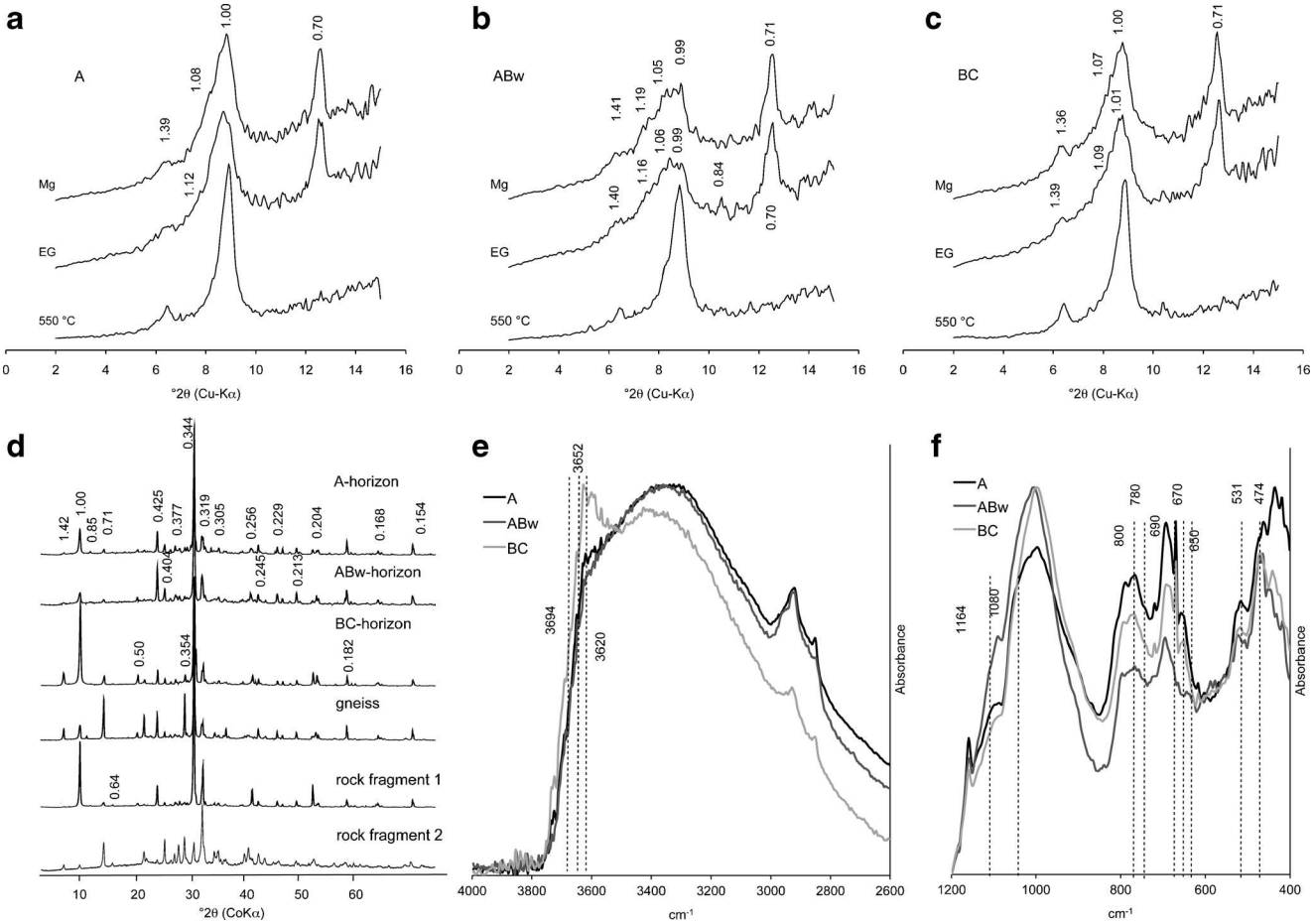

Fig. 8 Mineralogy of the soil profiles: X-ray patterns of the<1-μm fraction of the A, ABw and BC horizons. The XRD curves are corrected for Lorentz and polarisation factors and *d*-spacings are given in nm (**a**–**c**). Mg=Mg-saturated sample, EG=ethylene glycol solvation and corresponding heating treatment (550 °C). **d** X-ray data up to>60° 2θ from powder samples of the fine earth fraction (<2 mm) of the soil profile (A, ABw and BC horizon), rock fragments in the soil and the gneiss sample (Akkol river), (**e** and **f**) the FTIR spectra (absorbance) of the<2-mm fractions for the range 4,000–2,600 and 1,200–400 cm^{-1} with indication of peak positions

be further narrowed down to about 1,400–5,400 years. The rather low weathering stage of the soils is in agreement with these age indications.

5 Discussion

The investigated soils have a relatively young age and are consequently rather weakly developed. Nonetheless, active pedogenesis is taking place despite the harsh and very cold climatic conditions (Lessovaia and Polekhovsky 2009). The micromorphology predominantly showed (i) an accumulation of weakly and moderately decomposed remains of organic material, (ii) the formation of humus and (iii) an initial development of iron clots, films and ferruginous plasma in situ. The orientation of biotite particles, especially at the bottom of the profile, indicates that the parent substrate mostly shows a fluvial, subglacial origin and sluggish sedimentation. The proportion of biotite was slightly decreasing towards the surface of the soil which can be due to weathering processes or some inhomogeneities of the parent material. The mineralogy of fine-size fractions (<1 μm) showed the presence of chlorite, biotite and irregularly mixed-layered biotite–vermiculite (with a low proportion of vermicuite layers) which is in good agreement with the thin section data. Chlorite and biotite were both identified also in the rock fragments from the soil horizons. This indicated that glacier material is the main source of fine-size fraction of the soil. In addition, material from the river bank and adjacent slopes was interspersed with the glacially abraded material (as shown by the chlorite and mica proportion of the river bank and the rock fragments in the soil). The fine-size fraction finally was the most sensitive to weathering and pedogenesis. Biotite transformation into mixed-layered biotite–vermiculite having a minor proportion of vermiculite reflects first steps of weathering under acid conditions and cold environmental conditions (Vogt et al. 2010). In the studied soil profile, the most weathered horizon (from a mineralogical point of view) seems to be the ABw

Table 5 Total elemental contents (major components) in the fine earth of the LOI-free fraction (inorganic part; normalised to 100%)

Site	Depth (cm)	SiO_2 (%)	Al_2O_3 (%)	Fe_2O_3 (%)	CaO (%)	MgO (%)	MnO (%)	Na_2O (%)	K_2O (%)	TiO_2 (%)	P_2O_5 (%)
North-facing											
Alt 3	0–15	66.7	14.0	6.2	2.7	3.9	0.109	2.8	2.3	0.97	0.36
Alt 3	15–30	67.8	14.1	6.0	2.8	3.5	0.118	2.4	1.9	0.97	0.47
Alt 4	0–15	66.4	14.1	6.5	2.6	4.0	0.129	2.5	2.3	1.07	0.36
Alt 4	15–30	68.3	14.0	6.0	2.5	3.2	0.107	2.6	1.8	1.03	0.42
Alt 5	0–15	64.5	14.9	6.8	2.5	4.5	0.114	2.6	2.7	1.06	0.42
Alt 5	15–30	65.0	15.5	6.5	2.4	4.1	0.099	2.6	2.4	1.03	0.45
Alt 6	0–15	64.4	15.6	6.1	2.4	4.9	0.103	2.5	2.7	0.96	0.31
Alt 6	15–30	64.9	15.5	6.1	2.3	4.8	0.108	2.5	2.6	0.96	0.34
Alt 7	0–15	66.6	14.1	6.3	2.6	3.9	0.115	2.7	2.3	1.03	0.38
Alt 7	15–30	68.3	13.7	5.7	2.8	3.4	0.099	2.8	1.9	0.94	0.39
South-facing											
Alt 8	0–15	66.4	14.2	6.1	2.7	3.9	0.110	2.6	2.6	0.96	0.39
Alt 8	15–30	67.1	13.9	5.8	2.9	3.7	0.110	2.6	2.4	1.00	0.46
Alt 9	0–15	67.4	14.0	5.9	2.4	3.8	0.105	2.7	2.3	0.96	0.38
Alt 9	15–30	68.5	13.5	5.8	2.6	3.3	0.107	2.7	2.0	0.99	0.49
Alt 10	0–15	66.7	14.5	5.9	2.4	4.3	0.103	2.4	2.4	0.95	0.37
Alt 10	15–30	66.2	14.9	6.1	2.4	4.1	0.106	2.5	2.3	0.99	0.38
Alt 11	0–15	65.8	14.8	6.1	2.5	4.6	0.102	2.4	2.5	0.98	0.33
Alt 11	15–30	67.8	14.2	5.8	2.5	3.8	0.106	2.4	2.0	0.99	0.45
Alt 12	0–15	67.2	14.1	6.2	2.6	3.8	0.107	2.5	2.1	1.04	0.36
Alt 12	15–30	67.8	13.9	5.8	2.7	3.7	0.107	2.5	2.1	0.97	0.40
Profile/horizon											
A	5–19	67.0	13.9	6.3	2.5	3.8	0.116	2.6	2.3	1.07	0.37
ABw	19–27	65.8	15.2	6.3	2.5	4.0	0.111	2.5	2.2	1.02	0.46
BC	27–68	65.9	15.0	6.4	2.3	3.9	0.109	2.6	2.3	1.05	0.32

horizon. It might be that some aeolian inputs gave rise to a 'rejuvenation' of the uppermost soil horizon. Many experimental and field observations of permafrost conditions demonstrate active weathering, mineral transformation processes and changes in the structure of (clay) minerals (e.g. Konishchev and Rogov 1993; Lessovaia et al. 2012). Often, chlorite seems to be the first silicate mineral to disappear (Vogt et al. 2010). In a literature review, Vogt et al. (2010) showed that hornblende and biotite are the next silicates to be disintegrated and feldspar grains may be covered by yellowish

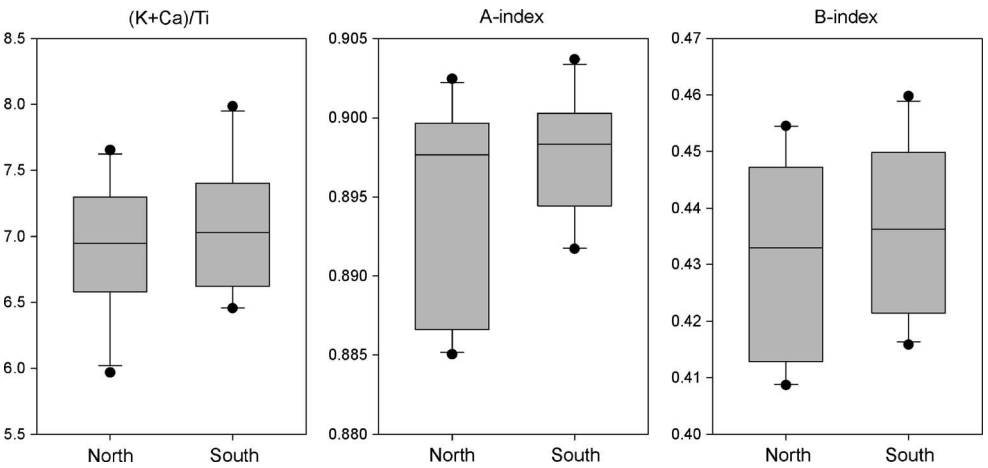

Fig. 9 Weathering indexes (A and B indexes; according to Kronberg and Nesbitt 1981) and (K+Ca)/Ti ratio as a function of exposure

Table 6 Radiocarbon dating of the stable organic carbon fraction (H_2O_2 treated sample) of an investigated soil and a nearby peat bog

Sample/site	Depth (cm)	UZH no	ETH no	Uncalibrated ages (yr uncal. BP)	$\partial^{13}C$ (‰)	Calibrated ages (yr cal BP) 2σ range
Peat (Alt 2)	60	6105	47904	585±30	−23.10±1.1	535–652
	100	6106	47905	1,485±30	−27.90±1.1	1,304–1,415
Soil, stable OM						
Alt 4	0–15	6103	48764	3,295±25	−26.11±1.1	3,453–3,579
Alt 4	15–30	6104	48765	4,665±25	−21.72±1.1	5,317–5,468

brown fine silty aggregates that are secondary clay minerals (Yershov 1998). At our sites, chlorite and mica reacted most. This can be explained by the selective destruction and transformation of such phyllosilicates in acidic soils of the northern taiga zone (Tonkonogov et al. 1987). Also smectites may be formed by mineral transformation reactions (Bender Koch et al. 1995; Falsone et al. 2012). Vogt et al. (2010) confirmed that cryogenic processes can be at least as efficient as those related to warm and temperate climates, with clay authigenesis being able to take place in relatively short periods of time. Consequently, the absence of smectitic clays in the studied soils confirms their week evolutional stage and indicates the relatively short time of pedogenesis.

The differences between north- and south-facing soils were astonishingly clear. Although the soils do not have a high age and are not very well developed, significant differences of pH, C and N concentrations and stocks, C/N ratio, the chemical structure of SOM and the Al_o, Fe_o, Al_d, Fe_d, Mn_o concentrations and stocks could be identified between the north- and south-exposure sites.

As regards the oxalate- and dithionite-extractable fractions of Al, in general, a slight concentration increase could be noted in the lower layer when compared to the surface layer. For Fe, both increase and decrease of the concentrations were measured. This increase in Al was more evident in the north-facing soils. This probably may point to the beginning of an eluvation or to inhomogeneities in the soil material (input of some aeolian material? or disturbances due to cryoturbation?).

Also due to the relatively young age, the C stocks in the soils are not very high (Fig. 5; average 6–8 kg C/m^2). The C abundance, however, only refers to a depth of 30 cm and probably covers only about 60–70% of the total mass. Arctic and subarctic lowland permafrost soils usually have higher organic carbon stocks. Hugelius and Kuhry (2009), for example, reported organic carbon stocks of 38 kg/m^2 (>100 cm soil depth) in taiga and tundra permafrost soils of northeastern European Russia. In northern circumpolar permafrost soils, Tarnocai et al. (2009) even found carbon abundances of 32.2–69.6 kg/m^2 (0–100 cm soil depth). Wetland conditions (water retention due to underlying permafrost or reduced evapotranspiration, peatland formation) and cryoturbation, particularly in permafrost soils, are major soil-forming processes in arctic and alpine regions and may contribute to a higher long-term storage of C in soils (Ugolini et al. 2006; Kaiser et al. 2007). Using the alpine soil chronofunctions given in Dahms et al. (2012) for Fe_o, Al_o, Mn_o and Si_o, the investigated soils here would fit very well for soils having age in the range of 1 to 10 kyr, which confirms their Holocene age.

Even though the climate can be classified as very harsh, the fact that chemical weathering seems to be more intense in the north-facing than in the south-facing soils fits with findings in the European Alps, where in well-developed (Egli et al. 2010) as well as young soils (Egli et al. 2006, 2011), distinct differences between north- and south-facing slopes were found. The evolution of soils, chemical weathering and formation and transformation of (clay) minerals always seemed to proceed faster on north-facing slopes. In several parts of the European Alps, eluviation and illuviation processes of Al and Fe—and consequently podzolisation processes—within a soil profile are more intense on north-facing slopes (Egli et al. 2010). Especially in the subalpine range, the stemflow as well as the accumulation of coniferous tree litter leads to an intensified acidification of the soil (Certini et al. 1998; Egli et al. 2010) and to a higher production of organic ligands in the soil solution. A higher amount of acid-soluble organic compounds and consequently —COOH functional groups was present on north-facing sites of the Italian Alps (Egli et al. 2010). Organic acids and ligands (Stumm and Wieland 1990; Lundström et al. 2000) particularly accelerate weathering processes on north-facing sites—not only in the European Alps but obviously also in the rather dry and very cold conditions of the Altai Mountains.

North-facing sites are characterised by lower temperatures, a lower evapotranspiration, a higher humidity and higher acidity. The higher humidity and the less favourable thermal conditions lead to an accumulation of labile, weakly degraded organic matter (e.g. as seen by the higher relative proportion of polysaccharides in the investigated north-facing soils; Fig. 6) and consequently to a higher production of soluble organic ligands and organic acids (higher proportion of carboxylic groups on north-facing sites; Fig. 6) that enhance weathering. This is in agreement with Ascher et al. (2012) who found that the $\delta^{13}C$ signatures of the PLFA (phospholipid fatty acid analysis) markers in alpine soils suggested a lower

decomposition rate at the cooler north-facing sites, resulting in a lower respiratory loss and an accumulation of weakly decomposed organic material. DGGE (denaturing gradient gel electrophoresis) data supported the PLFA results.

6 Conclusions

Coming back to the initially made hypothesis, we can confirm that even under very harsh and cold conditions the availability of water is crucial and that temperature, as a factor per se, seems to play a less important role. This statement partially fits with the hypothesis of Brantley et al. (2011; hypothesis no. 9) that the export of weathering products (and consequently weathering in general) predominantly depends on precipitation and evapotranspiration. This, however, may partially conflict with another hypothesis concerning the biota-facilitated chemical weathering (i.e. that the solar-to-chemical conversion of energy by plants controls the location and extent of biological weathering) given in Brantley et al. (2011).

Water availability predominantly determines weathering also in very cold regions of the Altai Mountains and agrees with results from the European Alps (Egli et al. 2006). Due to the less favourable thermal conditions, microbial activity is most likely reduced at north-facing sites (a hypothesis that still has to be tested and confirmed). This leads to an accumulation of labile, weakly degraded organic matter and consequently to a higher production of soluble organic ligands and organic acids. Together with the higher soil moisture, these circumstances enhance weathering mechanisms.

Acknowledgments The XRD measurements of the soil and rock samples were carried out at the X-ray Diffraction Centre of the St. Petersburg State University. This research was supported by a grant of the Scientific and Technological Cooperation Programme Switzerland–Russia.

References

Agatova AR, Hule VV, Mistrykov AA (2002) Dynamics of Sophiysky glacier (south-eastern Altay): the Late Glacial Maximum-XX century. Geomorphology (Geomorphologia) 2:92–105

Ascher J, Sartori G, Graefe U, Thornton B, Ceccherini MT, Pietramellara G, Egli M (2012) Are humus forms, mesofauna and microflora in subalpine forest soils sensitive to thermal conditions? Biol Fertil Soils 48:709–725

Bender Koch C, Mørup S, Madsen MB, Vistisen L (1995) Iron-containing weathering products of basalt in a cold, dry climate. Chem Geol 122:109–112

Birkeland PW (1999) Soils and geomorphology. Oxford University Press, New York

Brantley SL, Megonigal JP, Scatena FN, Balogh-Brunstad Z, Barnes RT, Bruns MA, van Cappellen P, Dontsova K, Hartnett HE, Hartshorn AS, Heimsath A, Herndorn E, Jin L, Keller CK, Leake JR, McDowell WH, Meinzer FC, Mozdzer TJ, Petsch S, Pett-Ridge J, Pregitzer KS, Raymond PA, Riebe CS, Shumaker K, Sutton-Grier A, Walter R, Yoo K (2011) Twelve testable hypotheses on the geobiology of weathering. Geobiology 9:140–165

Brindley GW, Brown G (1980) Crystal structures of clay minerals and their X-ray identification (Eds) Monograph 5, Mineralogical Society, London

Bronk Ramsey C (2001) Development of the radiocarbon calibration program OxCal. Radiocarbon 43:355–363

Bronk Ramsey C (2009) Bayesian analysis of radiocarbon dates. Radiocarbon 51:337–360

Carter BJ, Ciolkosz EJ (1991) Slope gradient and aspect effects on soils developed from sandstone in Pennsylvania. Geoderma 49:199–213

Certini G, Ugolini FC, Corti G, Agnelli A (1998) Early stages of podzolization under Corsican pine (*Pinus nigra* Arn. *ssp. laricio*). Geoderma 83:103–125

Conen F, Yakutin MV, Zumbrunn T, Leifeld J (2007) Organic carbon and microbial biomass in two soil development chronosequences following glacial retreat. Eur J Soil Sci 58:758–762

Cornell RM, Schwertmann U (2003) The iron oxides structure, properties, reactions, occurrences and uses, 2nd edn. Wiley-VCH GmbH & Co., Weinheim

Dahlgren RA, Boettinger JL, Huntington GL, Amundson RG (1997) Soil development along an elevational transect in the western Sierra Nevada, California. Geoderma 78:207–236

Dahms D, Favilli F, Krebs R, Egli M (2012) Soil weathering and accumulation rates of oxalate-extractable phases from alpine chronosequences of up to 1 Ma in age. Geomorphology 151–152: 99–113

Dixon JL, von Blanckenburg F (2012) Soils as pacemakers and limiters of global silicate weathering. CR Geosci 344:596–609

Dixon JL, Heimsath AM, Anmundson R (2009) The critical role of climate and saprolite weathering in landscape evolution. Earth Surf Proc Land 34:1507–1521

Dixon JL, Hartshorn AS, Heimsath AM, DiBiase RA, Whipple KX (2012) Chemical weathering response to tectonic forcing: a soils perspective from the San Gabriel Mountains, California. Earth Planet Sci Lett 323–324:40–49

Dokuchaev VV (1883) Russian Chernozem. In: Kaner N. (ed) Selected works of V. V. Dokuchaev (1967), Jerusalem, Int. Program Sci. Transl., pp 1–419

Egli M, Wernli M, Kneisel C, Haeberli W (2006) Melting glaciers and soil development in the proglacial area Morteratsch (Swiss Alps): I. Soil type chronosequence. Arch Antarct Alp Res 38:499–509

Egli M, Mirabella A, Sartori G, Giaccai D, Zanelli R, Plötze M (2007) Effect of slope aspect on transformation of clay minerals in alpine soils. Clay Miner 42:375–401

Egli M, Mirabella A, Sartori G (2008) The role of climate and vegetation in weathering and clay mineral formation in late Quaternary soils of the Swiss and Italian Alps. Geomorphology 102:307–324

Egli M, Sartori G, Mirabella A (2010) The effects of exposure and climate on the weathering of late Pleistocene and Holocene alpine soils. Geomorphology 114:466–482

Egli M, Wernli M, Burga C, Kneisel C, Mavris C, Valboa G, Mirabella A, Plötze M, Haeberli W (2011) Fast but spatially scattered smectite-formation in the proglacial area Morteratsch: an evaluation using GIS. Geoderma 164:11–21

Falsone G, Celi L, Caimi A, Simonov G, Bonifacio E (2012) The effect of clear cutting on podzolisation and soil carbon dynamics in boreal forests (Middle Taiga zone, Russia). Geoderma 177–178:27–38

Favilli F, Egli M, Cherubini P, Sartori G, Haeberli W, Delbos E (2008) Comparison of different methods of obtaining a resilient organic matter fraction in alpine soils. Geoderma 145:355–369

Gorbushina AA (2007) Life on the rocks. Minireview. Environ Microbiol 9:1613–1631

Hall K, Thorn CE, Matsuoka N, Prick A (2002) Weathering in cold regions: some thoughts and perspectives. Prog Phys Geogr 26: 577–603

Harnois L (1988) The CIW index: a chemical index of weathering. Sediment Geol 55:319–322
Harrington CD, Whitney JW (1987) Scanning electron microscope method of rock-varnish dating. Geology 15:967–970
Hitz C, Egli M, Fitze P (2002) Determination of the sampling volume for representative analysis of alpine soils. Z Pflanz Bodenkunde 165: 326–331
Hlavay J, Jonas K, Elek S, Inczedy J (1978) Characterization of the particle size and the crystallinity of certain minerals by IR spectrophotometry and other instrumental methods; II. Investigations on quartz and feldspar. Clays Clay Minerals 26:139–143
Hugelius G, Kuhry P (2009) Landscape partitioning and environmental gradient analyses of soil organic carbon in a permafrost environment. Global Biogeochem Cycle 23:GB3006
IUSS Working Group WRB (2007) World reference base for soil resources (2nd ed.). World Soil Resources Reports No. 103, First update, FAO, Rome
Jann B (2005) Einführung in die Statistik. 2. bearbeitete Auflage, Oldenburg Wissenschaftsverlag, München
Jenny H (1941) Factors of soil formation. Mc Graw-Hill Book Company, New York
Kaiser C, Meyer H, Biasi C, Rusalimova O, Barsukov P, Richter A (2007) Conservation of soil organic matter through cryoturbation in arctic soils in Siberia. J Geophys Res Biogeosci 112:G02017
Klemmedson JO (1964) Topofunction of soils and vegetation in a landscape. Am Soc Agron 5:176–189
Kloprogge JT, Hickey L, Frost RL (2004) FT-Raman and FT-IR spectroscopic study of the local structure of synthetic Mg/Zn/Al-hydrotalcites. J Raman Spectrosc 35:967–974
Konishchev VN, Rogov VV (1993) Investigations of cryogenic weathering in Europe and Northern Asia. Permafr Periglac 4:49–64
Kronberg GI, Nesbitt HW (1981) Quantification of weathering of soil chemistry and soil fertility. J Soil Sci 32:453–459
Langer K, Raith M (1974) Infrared spectra of Al-Fe(III)-epidotes and zoisites, $Ca_2(Al_{1-p}Fe^{3+}{}_p)Al_2O(OH)[Si_2O_7][SiO_4]$. Am Mineral 59: 1249–1258
Lanson B (1997) Decomposition of experimental X-ray diffraction patterns (profile fitting): a convenient way to study clay minerals. Clays Clay Minerals 45:132–146
Lessovaia SN, Polekhovsky YS (2009) Mineralogical composition of shallow soils on basic and ultrabasic rocks of east Fennoscandinavia and of the Ural Mountains, Russia. Clays Clay Minerals 57:476–485
Lessovaia S, Dultz S, Polekhovsky Y, Krupskaya V, Vigasina M, Melchakova L (2012) Rock control of pedogenic clay mineral formation in a shallow soil from serpentinous dunite in the polar Urals, Russia. Appl Clay Sci 64:4–11
Lorenzoni P, Mirabella A, Bidini C, Lulli L (1995) Soil genesis on trachytic and leucitic lavas of Cimini volcanic complex (Latium, Italy). Geoderma 68:79–99
Lundström US, van Breemen N, Bain D (2000) The podzolization process. A review. Geoderma 94:91–107
Macyk TM, Pawluk S, Lindsay D (1978) Relief and microclimate as related to soil properties. Can J Soil Sci 58:421–438
Madejova J, Komadel P (2005) Information available from infrared spectra of the fine fraction of bentonites. In: Kloprogge JT (ed) The application of vibration spectroscopy of clay minerals and layered double hydroxides, CMS workshop lectures, vol 13. The Clay Mineral Society, Aurora, CO, pp 65–98
Marinina AM, Samoilova GS (1987) Physical geography of the mountainous (Phizicheskaya geographiya Gornogo Altaya) Barnaul BGPE (in Russian)
Mavris C, Egli M, Plötze M, Blum JD, Mirabella A, Giaccai D, Haeberli W (2010) Initial stages of weathering and soil formation in the Morteratsch proglacial area (upper Engadine, Switzerland). Geoderma 155:359–371
McKeague JA, Brydon JE, Miles NM (1971) Differentiation of forms of extractable iron and aluminium in soils. Soil Sci Soc Am Proc 35: 33–38
Mehra OP, Jackson ML (1958) Iron oxide removal from soils and clays by a dithionite-citrate system buffered with sodium bicarbonate. Clay Clay Miner 7:317–327
Mizota C, van Reeuwijk LP (1989) Clay mineralogy and chemistry of soils formed in volcanic material in diverse climate regions. International Soil Reference and Information Centre, Soil Monograph, vol. 2, Wageningen
Moore DM, Reynolds RC (1997) X-ray diffraction and the identification and analysis of clay minerals, 2nd edn. Oxford University Press, New York, NY
Narozhniy Y, Zemtsov V (2011) Current state of the Altai Glaciers (Russia) and trends over the period of instrumental observations 1952–2008. Ambio 40:575–588
Nesbitt HW, Young GM (1989) Formation and diagenesis of weathering profiles. J Geol 97:129–147
Ogureeva GN (1980) Botanical geography of Altai (Botanicheskaya geographia Altaya). Nauka, Moscow (in Russian)
Osawa A, Zyryanova OA, Matsuura Y, Kajimoto T, Wein RW (eds) (2010) Permafrost ecosystems: Siberian larch forests, ecological studies, Vol. 209, Springer Science+Business Media B.V.
Osokina VG (managing ed), Babaeva LI, Sazonova TN, Fomichkina TM, Shevchenko MA, Prokudina TM, Volodina KA, Ivanova ES, Shestel TV (1993) Scientific climate handbook of the USSR. series 3, multi-annual data, part 1 – 6, issue 20, regions of Tomsk, Novosibirsk, Altai and province of Kemerovo. Directorate of Hydrometeorology, Hydrometeorological Centre of the West-Siberian territory, Hydrometeoisdat, Sankt-Petersburg (in Russian)
Ostanin OV, Mikhailov NN, Arkhipov SM (2004) Change of glaciers of south and central Altai from the end of XIX century and tendencies of its development in XXI (Izmenenie lednikov uuzhnogo e zentral'nogo Altaya s konza XIX v. e tendenzii ekh razvitiya v XXI v.) Geography and nature management of Siberia (Geographiya e prirodopol'zovabie Sibiri) 7:172-182, Barnaul (in Russian)
Piccolo A, Mirabella A (1985) Effetto di differenti estraenti inorganici e organici su alcune proprietà chimiche e chimico-fisiche di un acido umico. Annali dell'Istituto Sperimentale per lo Studio e Difesa Suolo 16:159–168
Rasmussen C, Brantley SL, Richter D, Blum A, Dixon J, White A (2011) Strong climate control on plagioclase weathering in granitic terrain. Earth Planetary Sci Lett 301:521–530
Rech JA, Reeves RW, Hendricks D (2001) The influence of slope aspect on soil weathering processes in the Springerville volcanic field, Arizona. Catena 43:49–62
Reimer PJ, Baillie MGL, Bard E, Bayliss A, Beck JW, Blackwell PG, Bronk Ramsey C, Buck CE, Burr GS, Edwards RL, Friedrich M, Grootes PM, Guilderson TP, Hajdas I, Heaton TJ, Hogg AG, Hughen KA, Kaiser KF, Kromer B, McCormac FG, Manning SW, Reimer RW, Richards DA, Southon JR, Talamo S, Turney CSM, van der Plicht J, Weyhenmeyer CE (2009) INTCAL09 and MARINE09 radiocarbon age calibration curves, 0–50,000 years cal BP. Radiocarbon 51:1111–1150
Schroeder PA (2002) Infrared spectroscopy in clay science. In: Rule A, Guggenheim S (eds) CMS workshop lectures, vol. 11, teaching clay science. The Clay Mineral Society, Aurora, CO, pp 181–206
Senesi N, D'Orazio V, Ricca G (2003) Humic acids in the first generation of EUROSOILS. Geoderma 116:325–344
Simas FNB, Schaefer CEGR, Melo VF, Guerra MBB, Saunders M, Gilkes RJ (2006) Clay sized minerals in permafrost-affected soils (Cryosols) from King George Island. Antarctica. Clays Clay Minerals 54:721–736
Stevenson FJ (1994) Humus chemistry: genesis, composition, reactions. Wiley, New York, NY

Stumm W, Wieland E (1990) Dissolution of oxide and silicate minerals: rates depend on surface speciation. In: Stumm W (ed) Aquatic chemical kinetics: reaction rates of processes in natural waters. Wiley-Interscience, New York, pp 367–398

Syromyatina MV (2010) Recent changes of climate and elements of high-altitude belts of Altai landscapes (Sovremennye izmeneneya klimata b elementov vysotnoi poyasnosti landshaftov Altaya). PhD thesis, St-Petersburg (in Russian)

Tan KH (2003) Humic matter in soil and the environment: principles and controversies. Marcel Dekker, Inc., New York – Basel

Tarnocai C, Canadell JG, Schuur EAG, Kuhry P, Mazhitova G, Zimov S (2009) Soil organic carbon pools in the northern circumpolar permafrost region. Global Biogeochem Cyles 23: GB2023

Tonkonogov VD, Gradusov BP, Rubilina NE, Targulian VO, Chizhikova NP (1987) On the differentiation of the mineralogical and chemical compositions of soddy podzolic and podzolic soils (K differenziazii mineralogicheskogo e khimicheskogo sostava dernovo-podzolistykh e podzolistykh pochv). Pochvovedenie 3:68–81 (in Russian)

Ugolini FC, Corti G, Certini G (2006) Pedogenesis in the sorted patterned ground of Devon plateau, Devon Island, Nunavut, Canada. Geoderma 136:87–106

Vantelon D, Pelletier M, Michot LJ, Barres O, Thomas F (2001) Fe, Mg and Al distribution in the octahedral sheet of montmorillonites. An infrared study in the OH-bending region. Clay Miner 36:369–379

Vogt T, Clauer N, Larqué P (2010) Impact of climate and related weathering processes on the authigenesis of clay minerals: examples from circum-Baikal region, Siberia. Catena 80:53–64

White AF, Blum AE (1995) Effects of climate on chemical weathering in watersheds. Geochim Cosmochim Acta 59:1729–1747

White AF, Blum AE, Bullen TD, Vivit DV, Schulz M, Fitzpatrick J (1999) The effect of temperature on experimental and natural chemical weathering rates of granitoid rocks. Geochim Cosmochim Acta 63:3277–3291

Whitney D, Evans BW (2010) Abbreviations for names of rock-forming minerals. Am Mineral 95:185–187

Williams JZ, Bandsra JZ, Pollard D, Brantley SL (2010) The temperature dependence of feldspar dissolution determined using a coupled weathering-climate model for Holocene-aged loess soils. Geoderma 156:11–19

Yershov ED (ed) (1998) General geocryology. Cambridge University Press, Cambridge

Zanelli R, Egli M, Mirabella A, Giaccai A, Abdelmoula M (2007) Vegetation effects on pedogenetic forms of Fe, Al and Si and on clay minerals in soils in southern Switzerland and northern Italy. Geoderma 141:119–129